[1]S. Doniach and B. A. Huberman, Phys. Rev. Lett. 42, 1169 (1979).
[2]B. I. Halperin and D. R. Nelson, Phys. Rev. Lett. 41, 121, 519(E) (1978), and to be published.
[3]A. L. Fetter and P. C. Hohenberg, Phys. Rev. 159, 330 (1967).
[4]A. T. Fiory, Phys. Rev. B 8, 5039 (1973).
[5]E. Conen and A. Schmid, J. Low Temp. Phys. 17, 331 (1974).
[6]J. M. Kosterlitz and D. J. Thouless, J. Phys. C 6, 1181 (1973).
[7]M. R. Beasley, J. E. Mooij, and T. P. Orlando, Phys. Rev. Lett. 42, 1165 (1979).
[8]B. I. Halperin and D. R. Nelson, to be published.
[9]V. K. Tkachenko, Zh. Eksp. Teor. Fiz. 50, 1573 (1966) [Sov. Phys. JETP 23, 1049 (1966)].
[10]P. Horn and R. D. Parks, Phys. Rev. B 4, 2178 (1972).

Effects on Photoemission of the Spatially Varying Photon Field at a Metal Surface

Harry J. Levinson and E. W. Plummer
Department of Physics and Laboratory for Research on the Structure of Matter, University of Pennsylvania, Philadelphia, Pennsylvania 19104

and

Peter J. Feibelman
Sandia Laboratories, Albuquerque, New Mexico 87185

(Received 18 July 1979)

Enhancement of photoionization cross sections due to spatially varying photon fields at a metal surface has been observed in the normal-emission cross sections for the surface state and Fermi level of Al(100) at photon energies between 9 eV and 23 eV. The data for Fermi-level photoexcitation are in excellent agreement with theoretical results for jellium. Below $\hbar\omega_p$, the predominant contribution to the photoionization matrix element comes from the spatially varying fields, which provide the momentum required for photoexcitation.

In this Letter we present unambiguous experimental evidence which shows that the spatially varying photon field at a metal surface must be taken into account in order to explain the magnitude and frequency dependence of energy- and angle-resolved photoionization cross sections. As seen in our data, this effect can be the dominant mechanism for photoexcitation. Since energy and momentum cannot be simultaneously conserved in photoexcitation from a translationally invariant electron gas, photoemission is usually attributed to the presence of a surface (the "surface photoeffect") or the lattice potential (the "bulk photoeffect"), either of which breaks translational symmetry and can provide the momentum necessary to overcome the kinematic restriction. However, the structure in our data cannot be explained in terms of either the surface barrier or lattice potential, and it is necessary to consider the spatially varying photon field at the surface[1-6] as a source of momentum.

The discussion of the photoeffect given above can be made precise by examining all of the contributions to the cross section for photoexcitation from an initial state ψ_i to a final state[7] ψ_f,

$$\frac{d\sigma}{d\Omega\, d\omega}=\frac{e^2}{\hbar c}\frac{\pi^2 k}{|\vec{A}_0|^2 m\hbar\omega}\left|\int \vec{j}_{fi}(\vec{r})\cdot\vec{A}(\vec{r})d^3r\right|^2, \qquad (1)$$

where $\vec{j}_{fi}(\vec{r})=\psi_f^*(\vec{r})\nabla\psi_i(\vec{r})-\psi_i(\vec{r})\nabla\psi_f^*(\vec{r})$ is the transition current density and $\vec{A}(\vec{r})$ is the vector potential of the photon field.[8] In approximating Eq. (1) it is usually assumed that the spatial dependence of $\vec{A}(\vec{r})$ can be neglected since the wavelength of the light is long compared with atomic dimensions. This leads to the familiar dipole matrix element which in a single-particle model may be written in terms of the crystal potential[7] $V(\vec{r})$:

$$\frac{d\sigma}{d\Omega\, d\omega}=\frac{e^2}{\hbar c}\frac{4\pi^2\hbar^2 k}{m\hbar\omega(E_f-E_i)^2}\left|\langle f|\vec{e}_A\cdot\nabla V(\vec{r})|i\rangle\right|^2. \qquad (2)$$

What ∇V does is to furnish the required momentum so that both energy and momentum can be conserved in photoexcitation. The assumptions leading to Eq. (2) are incorrect when the dielectric response of the solid to the incident electro-

magnetic radiation results in a vector potential varying rapidly in space (over atomic dimensions) near the surface. In that case $\vec{A}(\vec{r})$ may not be approximated by a constant and, consequently, the use of the dipole matrix element is invalid. Since only the perpendicular field components can vary rapidly, the dipole forms for the matrix element and dipole selection rules for photoexcitation by parallel field components remain applicable.[9]

Recent studies of the surface photoeffect, both experimental and theoretical, have considered the photon-energy dependence of the total photoyield from nearly-free-electron metals.[2-6,10] However, the interpretation of total photoyield data is difficult because of the large contributions due to secondary electrons and surface plasmons.[10] In our experiments we have utilized angle- and energy-resolved photoelectron spectroscopy to obtain a much more direct measurement of the surface photoeffect. In energy-resolved experiments the inelastic scattering of electrons is relevant only to the extent that it provides surface sensitivity. Angle-resolved detection with use of polarized light permits specific symmetry initial states and photon field components to be selected.[9]

Aluminum was chosen because it is a nearly-free-electron metal which has, on the (100) face, a surface state[11,12] that can easily be resolved from the inelastic background. We measured the area of the surface-state peak and the height of the Fermi edge, properly normalized to the incident photon flux,[13] as a function of photon energy. Both of these initial states are completely symmetric with respect to all symmetry operations of the surface and therefore the only electrons seen with collection normal to the surface are those excited by the component of the vector potential normal to the surface (A^z).[13] The final-state bands are such that no structure in the normal-emission data is attributable to direct transitions from the Fermi level.[14]

The data were taken with an angle-resolving spectrometer.[15] The angular resolution was $\pm 2.5°$ and the energy resolution 0.2 eV. All of the data shown were for normal-emission, p-polarized light incident at 45° in the (110) plane of the surface. Figure 1 shows the normal-emission cross sections for the surface state, 2.7 eV below the Fermi energy, and the Fermi edge, for two Al(100) crystals. For both initial states the cross section rises from threshold, peaks at 12.5 eV (photon energy), falls rapidly to a small value at

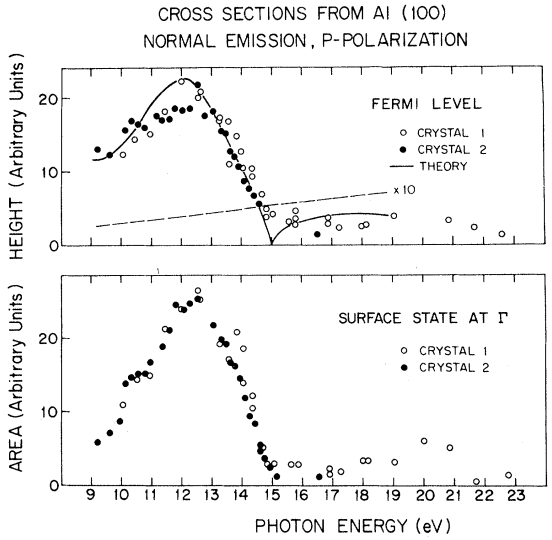

FIG. 1. The circles are the measured relative photoionization cross sections of the surface state and Fermi level. The solid line is the calculated Fermi-level cross section from jellium using self-consistently determined electromagnetic fields (Ref. 3) while the dashed line is the dipole cross section with use of a field of unit amplitude everywhere in space [$A(r) = 1$]. The $r_s = 2$ jellium calculations are plotted as a function of $\hbar\omega/\hbar\omega_p$, where $\hbar\omega_p$ is renormalized to the measured plasma energy of 15 eV.

the bulk plasma energy (15 eV), and remains small at higher photon energies. The magnitude of the enhanced cross section below the plasma energy can be illustrated by a direct comparison with the cross section for the d bands in a Ni(100) crystal. At $\hbar\omega = 12$ eV the height of the Ni d bands is 6 to 8 times larger than the Fermi edge in Al, but the reflectivity of Al is ~8 times larger than that of Ni. Therefore the height of the Fermi edge in Al is approximately the same as the height of the d bands in Ni per absorbed photon. In contrast at $\hbar\omega = 23$ eV the d bands of Ni are ~300 times larger than the Fermi edge in Al per absorbed photon.

The possibility of a final-state surface resonance causing the structure in the data can be eliminated because the photoelectrons are energy resolved. Given the nearly 3-eV difference in the binding energy of the two different initial states, the experimental observation that the maximum and minimum in their cross sections occur at the same photon energy rules out a final state at fixed kinetic energy. Moreover, there is no indication of structure in the secondary electrons at a fixed kinetic energy which is an indica-

tion of a final-state resonance.[16]

The solid line in Fig. 1 is the calculated photoionization cross section for states at the Fermi energy, using a self-consistent jellium model for Al.[17] There is excellent agreement between theory and experiment. When the cross section is calculated using a constant (unity) electromagnetic field [Eq. (2)] the dashed line in Fig. 1 is generated. Since a slowly varying cross section for a constant field is also obtained from a more realistic model of Al which includes ion cores,[18,19] the structure in the measured cross section is not a result of the band structure of Al. If the calculated cross section for constant field is multiplied by the intensity of either the internal or external classical Fresnel fields (Fig. 2), calculated from the measured optical constants,[20,21] it cannot reproduce the experimental features. The cross section predicted with use of the Fresnel fields is always larger at $\hbar\omega = 20$ eV than at $\hbar\omega = 12$ eV.

The drop in photoemission cross section for $\hbar\omega \to \hbar\omega_p$ can be understood as follows: normalizing to the classical (Fresnel) field inside the solid A_{cl}^z(inside), the photoemission matrix element may be decomposed according to

$$M_{fi} = \int dz \left(\frac{A^z(z)}{A_{cl}^z(z)} - 1 \right) j_{fi}(z) - \frac{1}{\hbar\omega} \int dz \, \frac{dV}{dz} \psi_f^* \psi_i . \quad (3)$$

Not far below ω_p, the first term of Eq. (3) dominates the second (which is the ordinary dipole term) by a factor of as much as 6, since at these frequencies the spatial variation of $A^z(z)$ is much more effective in providing the momentum necessary for photoemission than is dV/dz. As $\hbar\omega \to \hbar\omega_p$ (see Fig. 3), the distance over which $A^z(z)$ changes from its vacuum to its bulk value increases appreciably. Above ω_p the characteristic length for the spatial variation of $A^z(z)$ is the plasma wavelength, which again is long compared with the rise distance of $A^z(z)$ well below ω_p. Consequently, near and above ω_p, $j_{fi}(z)$ has a chance to complete a full oscillation before $[A^z(z)/A_{cl}^z(\text{inside}) - 1]$ falls to zero (cf. Fig. 3). The attendant cancellation in the integral reduces its value considerably, and reflects the physical fact that when $A^z(z)$ varies more slowly it is less able to provide the momentum required to effect photoemission. Since the first term of Eq. (3) is dominant below ω_p, a large drop in its value as $\omega \to \omega_p$ obviously results in a large drop in the cross section.

We have shown that photoemission is greatly enhanced below ω_p in Al, the enhancement occuring because of the rapidly varying photon field at the surface. Similar surface variations of the field certainly occur in more complicated solids and this should account for the enhancement in photoemission (below ω_p) from Cu(111) and Ni(111) surface states.[22]

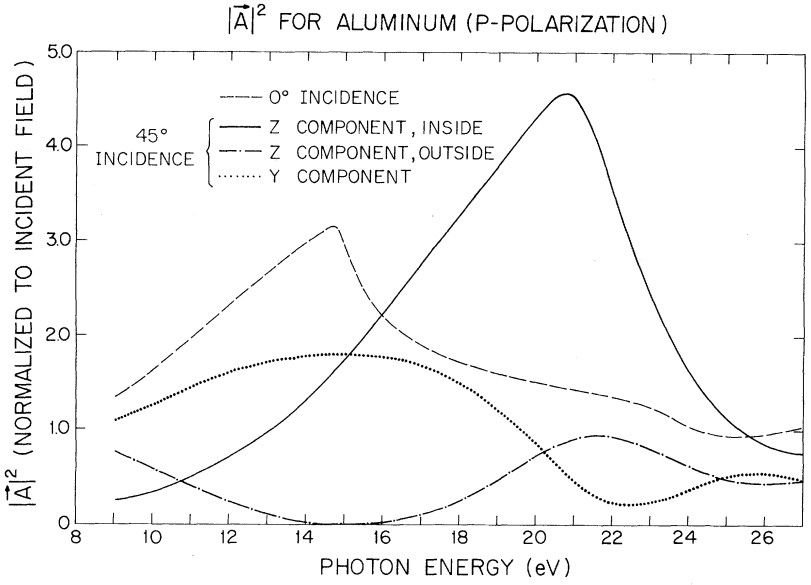

FIG. 2. Classical Fresnel electromagnetic fields. The y and z components are the parallel and normal components, respectively.

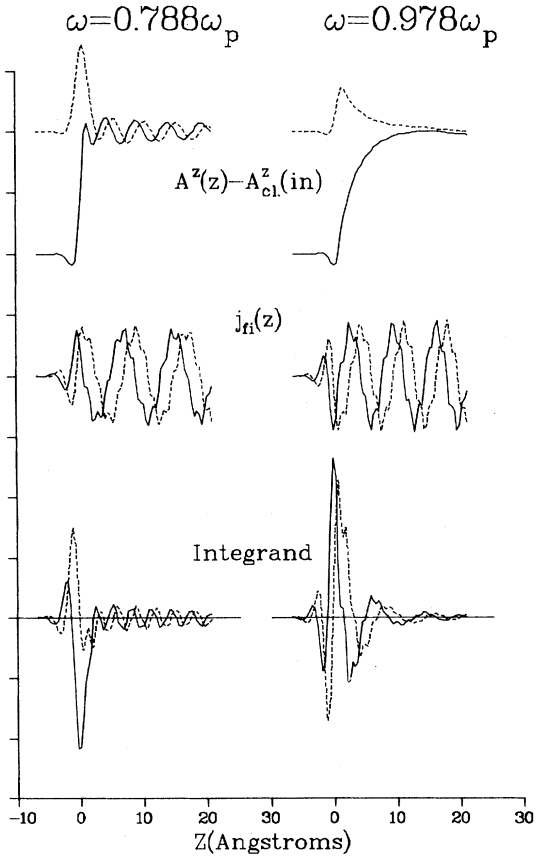

FIG. 3. Comparison of contributions to the photoemission matrix element because of the spatial variation of $A^z(z)$, for a frequency near the peak in the Fermi energy yield ($\omega = 0.788\omega_p$), and just below the plasma frequency ($\omega = 0.978\omega_p$). In each case solid and dashed lines correspond to real and imaginary part, respectively. The "integrand" is the product of the z component, $j_{fi}(z)$ and $A^z(z) - A_{cl}{}^z$(inside).

We wish to thank Dr. John B. Pendry for communicating unpublished data and G. Luckman for technical assistance. This work was supported by the National Science Foundation–Materials Research Laboratories Grant No. DMR 76-80994 and in part by U. S. Department of Energy No. DE-ACO4-76-DP00789. The Science Research Council at the University of Wisconsin was supported by National Science Foundation Grant No. 74-15098. Sandia Laboratories is a U. S. Department of Energy facility.

[1]R. E. B. Mackinson, Proc. Roy. Soc. London, Ser. A 162, 367 (1937).
[2]J. G. Endriz, Phys. Rev. B 7, 3464 (1973).
[3]P. J. Feibelman, Phys. Rev. Lett. 34, 1092 (1975), and Phys. Rev. B 12, 1319 (1975).
[4]K. L. Kliewer, Phys. Rev. B 14, 1412 (1976), and 15, 3759 (1977).
[5]G. Mukhopadhyay and S. Lundqvist, Phys. Scr. 17, 69 (1978).
[6]P. Apell, Phys. Scr. 17, 535 (1978).
[7]H. A. Bethe and E. E. Salpeter, *Quantum Mechanics of One and Two Electron Atoms* (Springer, Berlin, 1957), part IV.
[8]The continuum final states are normalized to δ functions in k space. We choose the gauge for which the scalar potential is zero everywhere.
[9]J. Hermanson, Solid State Commun. 22, 9 (1977).
[10]H. Petersen and S. B. M. Hagström, Phys. Rev. Lett. 41, 1314 (1978); H. Petersen, Z. Phys. B31, 171 (1978).
[11]P. O. Gartland and B. J. Slagsvold, Solid State Commun. 25, 489 (1978).
[12]G. V. Hansson and S. A. Flodstrom, Phys. Rev. B 18, 1562 (1978).
[13]The photon flux was measured using both sodium salicylate and a National Bureau of Standards Al_2O_3 calibrated photodiode, yielding nearly identical results. Second-order contributions were eliminated with use of an Al window.
[14]V. Hoffstein and D. S. Boudreaux, Phys. Rev. B 2, 3013 (1970).
[15]C. L. Allyn, T. Gustafsson, and E. W. Plummer, Rev. Sci. Instrum. 49, 1197 (1978).
[16]S.-L. Weng, E. W. Plummer, and T. Gustafsson, Phys. Rev. B 18, 1718 (1978).
[17]The method by which the fields are calculated is described at length in the second paper of Ref 3. A self-consistent $r_s = 2$ jellium surface potential barrier has been used. The calculated and measured cross sections were normalized at $\hbar\omega = 13$ eV.
[18]J. B. Pendry and J. F. L. Hopkinson, J. Phys. (Paris), Colloq. 7, C4-142 (1978).
[19]J. B. Pendry, private communication.
[20]H. J. Hagemann, W. Gudat, and C. Kunz, J. Opt. Soc. Am. 65, 742 (1978).
[21]R. W. Ditchburn and G. H. C. Freeman, Proc. Roy. Soc. (London) A294, 20 (1906).
[22]F. J. Himpsel and D. E. Eastman, Phys. Rev. Lett. 41, 507 (1978).